A Layer-Integrated Model of Solute Transport in Heterogeneous Media

Hung-En Chen[1], Hui-Ping Lee[1], Shih-Wei Chiang[2,*], Tung-Lin Tsai[3] and Jinn-Chuang Yang[4]

[1] *Department of Civil Engineering, National Chiao Tung University, 1001 Ta Hsueh Road, Hsinchu 30010, Taiwan*
[2] *Agricultural Engineering Research Center, 196-1 Chung Yuan Road, Chungli 32061, Taiwan*
[3] *Department of Civil and Water Resources Engineering National Chiayi University, 300 Syuefu Road, Chiayi 60004, Taiwan*
[4] *Department of Civil Engineering and Disaster Prevention and Water Environment Research Center, National Chiao Tung University, 1001 Ta Hsueh Road, Hsinchu 30010, Taiwan*

Abstract. This study presents a numerical solution to the three-dimensional solute transport in heterogeneous media by using a layer-integrated approach. Omitting vertical spatial variation of soil and hydraulic properties within each layer, a three-dimensional solute transport can be simplified as a quasi-three-dimensional solute transport which couples a horizontal two-dimensional simulation and a vertical one-dimensional computation. The finite analytic numerical method was used to discretize the derived two-dimensional governing equation. A quadratic function was used to approximate the vertical one-dimensional concentration distribution in the layer to ensure the continuity of concentration and flux at the interface between the adjacent layers. By integration over each layer, a set of system of equations can be generated for a single column of vertical cells and solved numerically to give the vertical solute concentration profile. The solute concentration field was then obtained by solving all columns of vertical cells to achieve convergence with the iterative solution procedure. The proposed model was verified through examples from the published literatures including four verifications in terms of analytical and experimental cases. Comparison of simulation results indicates that the proposed model satisfies the solute concentration profiles obtained from experiments in time and space.

---

*Corresponding author.
Email: swchiang.cv92g@nctu.edu.tw (S-W. Chiang)

1   Introduction

The major difficulty of groundwater solute transport simulation could be attributed to the large degree of heterogeneity in the subsurface. In reality, physical properties of subsurface porous media are spatially and temporally variable rather than homogeneous, and could be simply considered as a multi-layered system. Therefore, groundwater solute transport simulation is usually performed by employing the concept of multi-layered system if the spatial variability of soil and hydraulic properties can be negligible within each layer and the subsurface porous media can be assumed as a series of parallel homogeneous layers with finite thickness. In the past decades, a number of analytical or semi-analytical solutions to solute transport in multi-layered system have been developed by many investigators, including one-dimensional diffusion modeling [3, 19], one-dimensional advection-diffusion modeling [4, 11, 13, 17, 18] and two-dimensional advection-diffusion modeling [1, 24, 30, 31].

Although, analytical solutions are free from numerical dispersion and other truncation errors that are often observed in numerical simulations, the initial and boundary conditions are so limited that are not suitable for many practical problems. Therefore numerical methodology is more widely applied, and consequently a variety of numerical schemes, as reviewed by Zhao et al. [32], have been developed. On the other hand, a fully three-dimensional model, which can appropriately simulate the aforementioned solute transport, may be overwhelmed by the demand of a large number of nodes or elements to become impractical to solve. To overcome these disadvantages, some researchers introduced a multi-layered technique to simplify the three-dimensional computation processes by splitting the entire domain into a number of thin layers. The full three-dimensional simulation can be reduced to the combination of vertical one-dimensional and horizontal two-dimensional computations. It would disregard some noticed local features but significantly reduces the consumption of computational time to improve feasibility and practicability. This conceptual procedure was first used in coastal water simulation [7, 10, 12, 14] and was later adopted and applied in some fields such as open-channel flow applications [5, 9, 21, 28] and subsurface flow simulation [15, 22, 29]. A similar concept was also used to examine groundwater solute transport in heterogeneous media [8], where a hybrid model was constructed by applying the finite analytic method for the horizontal two-dimensional computation along with an analytical function for the vertical one-dimensional computation. Through a multi-layered procedure, the model is suitable for large-scale simulation and demonstrates both accuracy and efficiency compared with analytical solutions.

The purpose of this paper is to test the feasibility of the latter approach. A quasi-three-dimensional numerical model, based on the multi-layered technique, is proposed to deal with this subject. The fundamental concept of the adopted approach is similar to Kuo et al. [8], but we solve the vertical solute profile numerically by introducing a quadratic function instead of using an analytical solution. The newly-proposed model can relieve the limitation of Dirichlet type boundary conditions along the upper boundary and Neu-

mann type boundary conditions along the lower boundary embedded in the model by Kuo et al. [8]. In the following paragraphs, the framework for solute transport modeling and adopted numerical algorithm are first introduced. Subsequently, a three-dimensional solute transport problem with a patch source is applied to verify the proposed model as well as to evaluate the effect of layer numbers on computational accuracy. Two heterogeneous media cases, respectively, with horizontal and vertical flow are then introduced to examine the reliability of numerical model. Finally, the numerical results are compared with experimental data to demonstrate the capabilities of the model.

2 Mathematical model

2.1 Governing equation

The three-dimensional mathematical model for solute transport processes in porous media without chemical reaction can be expressed as

$$\frac{\partial C}{\partial t}+u\frac{\partial C}{\partial x}+v\frac{\partial C}{\partial y}+w\frac{\partial C}{\partial z}=\frac{\partial}{\partial x}\left(D_x\frac{\partial C}{\partial x}\right)+\frac{\partial}{\partial y}\left(D_y\frac{\partial C}{\partial y}\right)+\frac{\partial}{\partial z}\left(D_z\frac{\partial C}{\partial z}\right), \qquad (2.1)$$

where t is the time; x, y and z are the Cartesian coordinates; C is the concentration of solute at location (x, y, z); D_x, D_y and D_z are the dispersivity coefficients; u, v and w denote velocity components in the directions x, y and z, respectively.

2.2 Layer-integrated equation

A sketch illustrating the layer division and the definition of coordinates for the computational domain in total K layers is shown in Fig. 1. Under the assumption of uniform soil properties in the vertical direction for each layer, the layer-averaged transport equation with regard to the kth layer can be obtained from integrating the governing equation
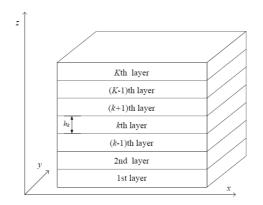

Figure 1: Schematic illustration of layer division and the definition of coordinates.

vertically over the layer from the bottom to the top and can be expressed as

$$\varphi_k = \frac{1}{h_k} \int_{z_{k-1/2}}^{z_{k+1/2}} \varphi(x,y,z,t)dz, \tag{2.2}$$

where the subscript k represents the average quantities over the kth layer; the supplementary subscripts $+1/2$ and $-1/2$ denote the quantities at top and bottom of the kth layer, respectively; φ_k represents the average physical variables for the kth layer such as u, v, w and C; $z_{k\pm1/2}$ represents the vertical elevations at top and bottom of the kth layer interfaces, respectively; h_k is the thickness of the kth layer. The governing equation for solute transport is integrated through K layers by applying Eq. (2.2) and Leibnizs rule. The layer-integrated formulation of the transport equation for the kth layer then gives

$$h_k\frac{\partial C_k}{\partial t} + u_k h_k \frac{\partial C_k}{\partial x} + v_k h_k \frac{\partial C_k}{\partial y} + w_k C_{k+1/2} - w_k C_{k-1/2}$$

$$= D_{x,k} h_k \frac{\partial^2 C_k}{\partial x^2} + D_{y,k} h_k \frac{\partial^2 C_k}{\partial y^2} + D_{z,k} \frac{\partial C}{\partial z}\Big|_{k+1/2} - D_{z,k} \frac{\partial C}{\partial z}\Big|_{k-1/2}. \tag{2.3}$$

2.3 Formulation of layer interface relation

The three-dimensional solute transport equation has been simplified as the layer-averaged form in xy two-dimensional subdomains, as given in Eq. (2.3). However, two more unknowns are produced at the top and bottom interfaces of each layer, e.g., $C_{k+1/2}$ and $C_{k-1/2}$ with respect to the kth layer. In addition, the vertical gradient values of $C_{k+1/2}$ and $C_{k-1/2}$ should be determined first. In this study, the concentration variation in the layer was modeled by a quadratic polynomial interpolation function, which was also adopted by Tsai et al. [25] for solving the advection-diffusion equation and Hung et al. [5] for shallow water free-surface flow computation. The quadratic function for solute concentration in each layer along z direction can be represented as

$$C(z) = a + bz + cz^2, \tag{2.4}$$

where a, b and c are undetermined coefficients. Applying the concentration values at the top and bottom interfaces

$$C(z=h_k) = a + bh_k + ch_k^2 = C_{k+1/2}, \tag{2.5a}$$
$$C(z=0) = a = C_{k-1/2}, \tag{2.5b}$$

together with the definition of C_k

$$C_k = \frac{1}{h_k} \int_0^{h_k} (a + bz + cz^2)dz, \tag{2.6}$$

the coefficients a, b and c in Eq. (2.4) can then be specified as follows

$$a = C_{k-1/2}, \tag{2.7a}$$

$$b = \frac{1}{h_k}(-2C_{k+1/2} + 6C_k - 4C_{k-1/2}), \tag{2.7b}$$

$$c = \frac{1}{h_k}(3C_{k+1/2} - 6C_k + 3C_{k-1/2}). \tag{2.7c}$$

By taking the first derivative of Eq. (2.4) with respect to z, the vertical gradient values of solute concentration at the top and bottom interfaces of the kth layer can be respectively expressed as

$$\left.\frac{\partial C}{\partial z}\right|_{k+1/2} = \frac{1}{h_k}(4C_{k+1/2} - 6C_k + 2C_{k-1/2}), \tag{2.8a}$$

$$\left.\frac{\partial C}{\partial z}\right|_{k-1/2} = \frac{1}{h_k}(-2C_{k+1/2} + 6C_k - 4C_{k-1/2}). \tag{2.8b}$$

Substituting Eqs. (2.8a) and (2.8b) into Eq. (2.3) yields the following form of equation:

$$h_k \frac{\partial C_k}{\partial t} + u_k h_k \frac{\partial C_k}{\partial x} + v_k h_k \frac{\partial C_k}{\partial y} + w_k C_{k+1/2} - w_k C_{k-1/2}$$
$$= D_{x,k} h_k \frac{\partial^2 C_k}{\partial x^2} + D_{y,k} h_k \frac{\partial^2 C_k}{\partial y^2} + \frac{D_{z,k}}{h_k}\left(6C_{k+1/2} - 12C_k + 6C_{k-1/2}\right). \tag{2.9}$$

2.4 External boundary conditions

The external boundary conditions can be expressed by given concentration or dispersive flux at any given time and can be given as any one of the following:

$$C|_{boundary} = C_0(t), \tag{2.10a}$$

$$D\frac{\partial C}{\partial n}\bigg|_{boundary} = Q_0(t), \tag{2.10b}$$

$$V_n C|_{boundary} - D\frac{\partial C}{\partial n}\bigg|_{boundary} = V_n C_0(t), \tag{2.10c}$$

where the subscript boundary represents the domain boundary; D is the dispersivity coefficient; n is the normal direction; V_n is the velocity component along the normal direction; $C_0(t)$ and $Q_0(t)$ are the known time-varying functions representing the specific concentration and dispersive flux, respectively.

2.5 Internal boundary conditions

The internal boundary conditions express the solute concentration relationship at each interface of neighboring two layers. The solute concentration and its gradient at each

layer interface should be continuous and can be shown in the following equations:

$$C_{k+1/2} = C_{(k+1)-1/2},$$ (2.11a)

$$\varepsilon_{z,k} D_{z,k} \frac{\partial C_{k+1/2}}{\partial z} = \varepsilon_{z,k+1} D_{z,k+1} \frac{\partial C_{(k+1)-1/2}}{\partial z},$$ (2.11b)

where ε represents the porosity of soil.

3 Numerical algorithm

3.1 Finite analytic formulation

In each layer, the finite analytic (FA) method was chosen to solve the transport equation. FA method was first introduced by Chen et al. [2] to perform two-dimensional fluid flow and heat transfer simulation and was applied to solute transport simulation to acquire convincing results [6,26,27]. The development history and engineering applications were further illustrated and reviewed by Lin et al. [16]. Applying the FA method at each time step, Eq. (2.9) for the kth layer at a node i, j can be specified as

$$\left(\frac{-6C_p}{h_k^2} \frac{D_{z,k}}{D_{x,k}} - \frac{C_p w_k}{D_{x,k} h_k} \right) C_{i,j,k-1/2}^{n+1} + \left(1 + \frac{C_p}{\Delta t D_{x,k}} + \frac{12C_p}{h_k^2} \frac{D_{z,k}}{D_{x,k}} \right) C_{i,j,k}^{n+1}$$

$$+ \left(\frac{-6C_p}{h_k^2} \frac{D_{z,k}}{D_{x,k}} + \frac{C_p w_k}{D_{x,k} h_k} \right) C_{i,j,k+1/2}^{n+1}$$

$$= C_{ne} C_{i+1,j+1,k}^{n+1} + C_{nw} C_{i-1,j+1,k}^{n+1} + C_{se} C_{i+1,j-1,k}^{n+1} + C_{sw} C_{i-1,j-1,k}^{n+1}$$

$$+ C_{wc} C_{i-1,j,k}^{n+1} + C_{ec} C_{i+1,j,k}^{n+1} + C_{nc} C_{i,j+1,k}^{n+1} + C_{sc} C_{i,j-1,k}^{n+1} + \frac{C_p}{D_{x,k} \Delta t} C_{i,j,k}^n,$$ (3.1)

where the superscripts n and $n+1$ are the time steps; C_{ne}, C_{nw}, C_{se}, C_{sw}, C_{wc}, C_{ec}, C_{nc}, C_{sc} and C_p are the FA coefficients. The detailed derivations of Eq. (3.1) are given in the Appendix.

3.2 Formation of algebraic system of equations

Applying Eq. (3.1) to a single column of vertical cells from bottom upward to top of the computational domain layer by layer, there are K layer-averaged transport equations can be produced for the K layers. Coupling with the bottom and top external boundary conditions and $(K-1)$ internal conditions, a set of algebraic system of equations consisting of $(2K+1)$ equations can be established and form a well-posed problem for a single column of vertical cells. Therefore, the total $(2K+1)$ undetermined unknowns can be solved by the $(2K+1)$ equations.

The computational procedure is illustrated as a flowchart shown in Fig. 2 and can be summarized in the following:
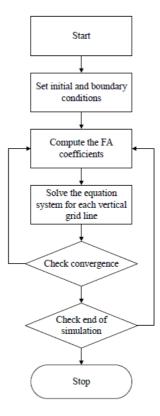
Figure 2: Flow chart of the computational procedure.

(a) Set the initial and boundary conditions for the domain of interest.

(b) Compute the FA coefficients.

(c) Solve the equations to obtain solute concentration distribution for each column of vertical cells.

(d) Repeat steps (b) and (c) if solute concentration does not converge for the whole computational domain.

(e) March through time by repeating steps (b) to (d).

4 Model verification

4.1 Solute transport with a patch source

Three-dimensional solute transport from a patch source in the unidirectional flow field illustrated in Fig. 3 is considered in this examination, for which the following initial con-
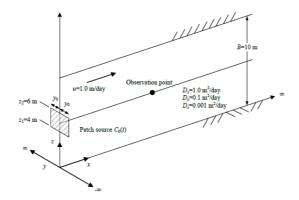
Figure 3: Schematic representation of solute transport with a patch source in unidirectional flow field.

dition applies

$$C(x,y,z,0)=0. \tag{4.1}$$

The boundary conditions are:

Left: $C(0,y,z,t)=\begin{cases} C_0(t), & -y_0<y<y_0 \text{ and } z_1<z<z_2, \\ 0, & \text{otherwise}, \end{cases}$ Right: $C(\infty,y,z,t)=0$, (4.2a)

Upper: $C(x,-\infty,z,t)=0$, Lower: $C(x,\infty,z,t)=0$, (4.2b)

Top: $\partial C(x,y,H,t)/\partial z=0$, Bottom: $\partial C(x,y,0,t)/\partial z=0$. (4.2c)

The analytical solution by Neville [20] is:

$$C(x,y,z,t)=\frac{x}{4H\sqrt{\pi D_x}}\int_0^t C_0(t-\xi)\frac{1}{\xi^{3/2}}\exp\left[-\lambda\xi-\frac{(x-u\xi)^2}{4D_x\xi}\right]\left[erfc\left(\frac{y-y_0}{2\sqrt{D_y\xi}}\right)\right.$$
$$\left.-erfc\left(\frac{y+y_0}{2\sqrt{D_y\xi}}\right)\right]\left\{(z_2-z_1)+\frac{2H}{\pi}\sum_{n=1}^{\infty}\frac{1}{n}\left[\sin\left(\frac{n\pi z_2}{H}\right)\right.\right.$$
$$\left.\left.-\sin\left(\frac{n\pi z_1}{H}\right)\right]\cos\left(\frac{n\pi z}{H}\right)\exp\left(-D_z\frac{n^2\pi^2}{H^2}\xi\right)\right\}d\xi, \tag{4.3}$$

where H is the aquifer thickness, λ is the reaction rate and $C_0(t)$ is the inflow concentration at the left boundary within the patch from $-y_0$ to y_0 and z_1 to z_2 (see Fig. 3). The constant concentration $C_0(t)=1$ with dispersivity $D_x=1$ is assumed to be released from the left boundary with the patch source of 2m in height and 2m in width. The parameters and soil properties used in the modeling are listed in Table 1. In order to investigate the effects of layer numbers on computational accuracy, $K=40$, $K=20$ and $K=10$ were applied to this case. At $x=10$m, the relative concentration (C/C_0) distributions along z direction for $t=5$ day, $t=10$ day and $t=30$ day are shown in Fig. 4 where the solid line is due to (4.3) and the symbols are due to our numerical solution. The results of the

Table 1: Summary of parameters for solute transport with a patch source.

	Symbol	Value	Unit
Time step	Δt	0.1	day
Space interval	$\Delta x, \Delta y$	0.1	m
Layer thickness	h_k	0.25	m
Layer number	K	40	-
Initial solute concentration	C_{ini}	0	-
Aquifer thickness	H	10	m
Reaction rate	λ	0	day^{-1}
	u	1	m day^{-1}
Seepage velocity	v	0	m day^{-1}
	w	0	m day^{-1}
Dispersivity coefficient	D_x	$\begin{bmatrix} 0.002 \\ 0.01 \\ 0.1 \\ 1 \end{bmatrix}$	$\text{m}^2\,\text{day}^{-1}$
	D_y	0.1	$\text{m}^2\,\text{day}^{-1}$
	D_z	0.1	$\text{m}^2\,\text{day}^{-1}$
Constant source concentration	C_0	1	-
Width of patch source	y_0	1	m
Position of patch source	z_1	4	m
	z_2	6	m

numerical simulation are in good agreement with those obtained by the analytical analysis for various layer numbers. Taking the results at $z=5$m after 30 days for example, a relative concentration of 0.1658 is obtained from the analytical solution while the numerical model yields 0.1657, 0.1655 and 0.1646 with $K=40$, $K=20$ and $K=10$, respectively. Using more layers cannot much improve the accuracy of results. It is that the relative CPU time (i.e., the CPU time relative to the case with $K=10$) consumed in simulation increases drastically as number of layers increases: 3.66 and 15.25 for $K=20$ and $K=40$, respectively for the cases studied.

　　With all other parameters remaining the same as previous section, the dispersivity D_x is set to 1, 0.01, and 0.002 to produce Peclet numbers (Pe) of 0.1, 10 and 50, respectively. Fig. 5 shows plots of the concentration profile in the longitudinal direction with $K=20$ at each Peclet number for $t=5$ day, $t=10$ day and $t=30$ day. With Peclet number of 10, some degree of numerical overshooting can be found in Fig. 5(b) and numerical oscillation occurs once the Peclet number is elevated to 50 (see Fig. 5(c)). It can be concluded from Fig. 5 and Fig. 4(b) ($Pe=1$) that the simulated results are worse with smaller dispersivity, i.e., larger Peclet number.

4.2　Horizontal solute transport in multi-zone heterogeneous media

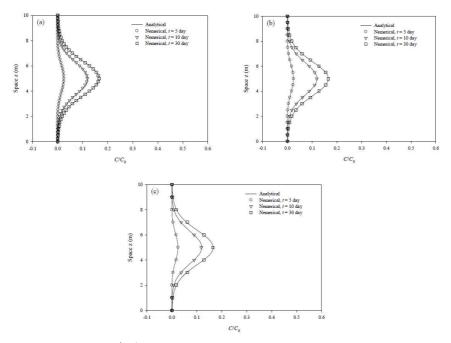One-dimensional solute transport in heterogeneous porous media under the condition of

Figure 4: Relative concentration (C/C_0 distribution along z direction for $t=5$ day, $t=10$ day and $t=30$ day from modeling with (a) $K=40$; (b) $K=20$; and (c) $K=10$.
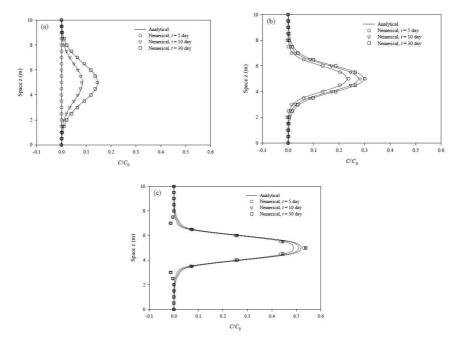
Figure 5: Relative concentration (C/C_0) distribution along z direction for $t=5$ day, $t=10$ day and $t=30$ day from modeling with (a) $Pe=0.1$; (b) $Pe=10$; and (c) $Pe=50$.
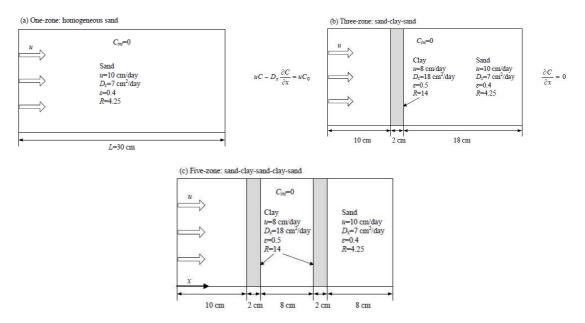
Figure 6: Schematic representation of one-dimensional solute transport in porous media with (a) one-zone (homogeneous sand); (b) three-zone (sand-clay-sand); and (c) five-zone (sand-clay-sand-clay-sand).

steady-state horizontal flow shown in Fig. 6 is considered in this examination. Liu et al. [17] derived an analytical solution for this problem by using a generalized integral transform method. In their study, three cases including one-zone case with a 30-cm-thick homogeneous sand soil, three-zone case with a 2-cm-thick clay zone placed in the center of the homogeneous sand soil and five-zone case with two separate 2-cm-thick clay zones placed in the sand soil (see Figs. 6(a), (b) and (c)) were taken into account respectively. The analytical solution is used to verify the numerical model proposed in this study under the same initial and boundary conditions shown in Fig. 6 along with the related soil parameters listed in Table 2. The comparisons of the analytical and numerical

Table 2: Summary of soil properties for horizontal solute transport in heterogeneous media.

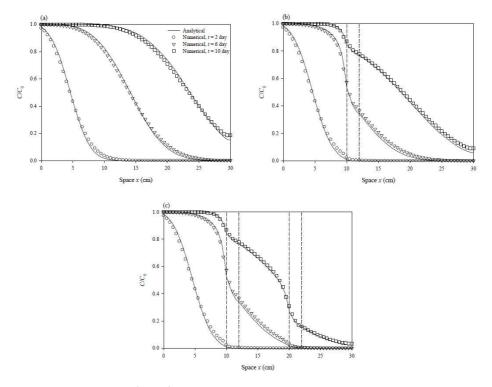|	Symbol	Value	Unit
Sand			
Velocity	u	10	cm day^{-1}
Dispersivity coefficient	D_x	7	cm^2 day^{-1}
Porosity	ε	0.4	-
Retardation factor	R	4.25	-
Clay			
Velocity	u	8	cm day^{-1}
Dispersivity coefficient	D_x	18	cm^2 day^{-1}
Porosity	ε	0.5	-
Retardation factor	R	14	-

Figure 7: Relative concentration (C/C_0) distribution along x direction for $t=2$ day, $t=6$ day and $t=10$ day in porous media with (a) one zone; (b) three-zone; and (c) five-zone.

solutions with one-zone, three-zone and five-zone cases are shown in Fig. 7 for three time periods, i.e., $t=2$ days, $t=6$ days and $t=10$ days.

The results in Fig. 7 present how solute transport is retarded by the existence of low-permeable clay layers and also show satisfactory agreement between the analytical and simulated results.

4.3 Vertical solute transport in two-layer heterogeneous media

To verify the vertical transport behavior, one-dimensional vertical solute transport in two-layered porous media with steady flow shown in Fig. 8 is studied herein. A zero initial concentration $C_{ini}=0$, constant inlet concentration $C_0(t)=1$ and constant outlet concentration $C_H(t)=0$ are given for this problem. The analytical solution of two-layered application has been reported by Li and Cleall [13], in which the soil properties for the inlet layer were assumed to be fixed while one of the following three parameters of dispersivity coefficient, porosity and retardation factor was varied with the others remaining unchanged for the outlet layer. The detailed soil parameters for these three scenarios are summarized in Table 3. Two-year simulation with the effects of various dispersivity coefficients, porosities and retardation factors on the solute concentration profiles are p-
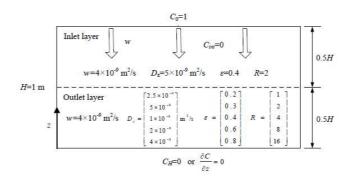
Figure 8: Schematic representation of one-dimensional vertical solute transport in two-layer porous media and related coefficients.

resented in Figs. 9(a), (b) and (c), respectively. It is seen in Fig. 9 that the simulated results are in good agreement with those obtained from the analytical solution.

The results for the same cases, but now considering a Neumann outlet condition (i.e., $\partial C/\partial z = 0$) are presented in Fig. 10, where it is seen that the solute concentration distributions obtained from analytical and numerical methods are in good agreement as well.

Table 3: Summary of soil properties for vertical solute transport in heterogeneous media.

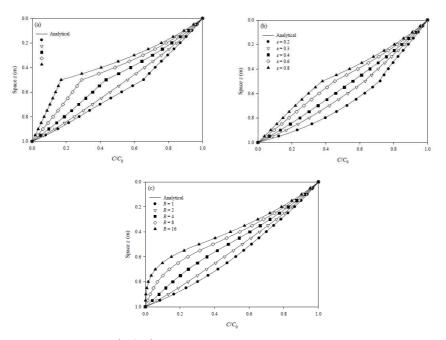|	Symbol	Value	Unit
Inlet layer			
Velocity	w	4×10^{-9}	m s^{-1}
Dispersivity coefficient	D_z	5×10^{-9}	m^2 s^{-1}
Porosity	ε	0.4	-
Retardation factor	R	2	-
Outlet layer			
Velocity	w	410^{-9}	m s^{-1}
Dispersivity coefficient	D_z	$\begin{bmatrix} 2.5 \times 10^{-9} \\ 5 \times 10^{-9} \\ 1 \times 10^{-8} \\ 2 \times 10^{-8} \\ 4 \times 10^{-8} \end{bmatrix}$	m^2 s^{-1}
Porosity	ε	$\begin{bmatrix} 0.2 \\ 0.3 \\ 0.4 \\ 0.6 \\ 0.8 \end{bmatrix}$	-
Retardation factor	R	$\begin{bmatrix} 1 \\ 2 \\ 4 \\ 8 \\ 16 \end{bmatrix}$	-

Figure 9: Relative concentration (C/C_0) distribution along z direction under Dirichlet outlet condition with various values of (a) dispersivity coefficient; (b) porosity; and (c) retardation factor.
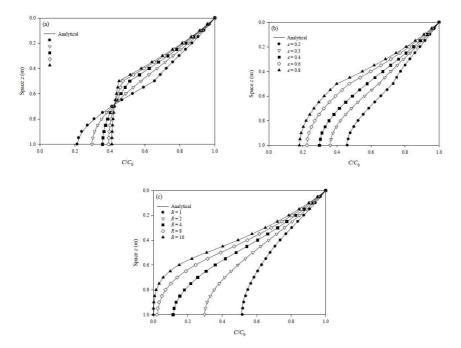

Figure 10: Relative concentration (C/C_0) distribution along z direction under Neumann outlet condition with various values of (a) dispersivity coefficient; (b) porosity; and (c) retardation factor.

It seems that the proposed model can properly simulate the concentration variation in two-layer heterogeneous media under various boundary conditions.

4.4 Solute transport in three-layer heterogeneous media

The numerical solution is compared to the experimental data from Sudicky et al. [23] to further test the proposed model. Sudicky et al. [23] conducted laboratory experiments by injecting a sodium chloride solution into a thin sand layer bounded by silt layers within a Plexiglass box (1.0m in length, 0.2m in thickness and 0.1m in width) as shown in Fig. 11. Two experiments were performed in the study, i.e., a continuous injection with flow velocity of 0.1m/day and an injection duration of 7 days with flow velocity of 0.5m/day respectively applied in the sand layer. The relevant parameters employed in the experiment are summarized in Table 4. Figs. 12 and 13 show the comparison between the numerical results and the experimental data for the variation of relative concentration with respect to time at the effluent end. Both of the two cases appear to be in reasonable agreement with the observed data though the numerical model gives a slight overestimation at some time spans.
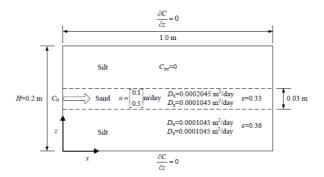

Figure 11: Schematic representation of solute transport in stratified porous media.
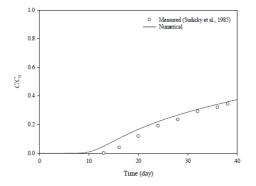

Figure 12: Comparison between numerical results and measurements for velocity of 0.1m/day.
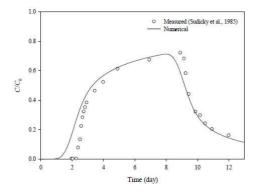
Figure 13: Comparison between numerical results and measurements for velocity of 0.5m/day.

Table 4: Summary of soil properties for solute transport in stratified porous media.

	Symbol	Value	Unit
Sand			
Velocity	u	$\begin{bmatrix} 0.1 \\ 0.5 \end{bmatrix}$	m day^{-1}
Dispersivity coefficient	D_x	0.0002045	m^2 day^{-1}
Dispersivity coefficient	D_z	0.0001045	m^2 day^{-1}
Porosity	ε	0.33	-
Clay Velocity	u	0	m day^{-1}
Dispersivity coefficient	D_x	0.0001045	m^2 day^{-1}
Dispersivity coefficient	D_z	0.0001045	m^2 day^{-1}
Porosity	ε	0.36	-

5   Conclusions

We presented and tested a numerical model for three-dimensional solute transport in porous media using a separate, but coupled, solution strategy for horizontal and vertical transport. By solving the vertical solute profile numerically instead of using an analytic solution (Kuo et al. 2008), we removed many of the restrictions on boundary conditions imposed by the analytic solution. The hybrid approach is accomplished by subdividing an aquifer in number of hypothetical layers in each of which horizontal transport is solved using the finite analytic method. These same layers form the basis for the numerical vertical transport calculations.

Verifications were carried out by comparison with analytical solutions and experimental results, which showed a good agreement between vertical concentration profiles. A varying number of layers were examined to investigate their effect on computational accuracy. We found that no appreciable improvement in accuracy was obtained with more layers, while the computational effort became burdensome if not impractical. We also tested different types of boundary conditions, including Dirichlet and Neumann conditions. Here the numerical results corresponded well with an analytic solution to a

two-layer aquifer system.

Overall, our tests showed that the proposed model is computationally efficient, reasonably accurate, and accommodates various boundary conditions.

Appendix

The appendix shows the derivations of discretization of solute transport equation by applying FA method.

Eq. (2.9) should be first expressed in a FA standard form as

$$2A\frac{\partial C_k}{\partial x} + 2BC\frac{\partial C_k}{\partial y} = \frac{\partial^2 C_k}{\partial x^2} + C\frac{\partial^2 C_k}{\partial y^2} - G, \tag{A.1}$$

in which

$$A = \frac{u_k}{2D_{x,k}}, \quad B = \frac{v_k}{2D_{y,k}}, \tag{A.2a}$$

$$C = \frac{D_{y,k}}{D_{x,k}}, \quad G = R\left(\frac{C_k^{n+1} - C_k^n}{\Delta t}\right) + f_p, \tag{A.2b}$$

$$R = \frac{1}{D_{x,k}}, \quad f_p = \frac{\frac{D_{z,k}}{h_k}\left(-6C_{k+1/2} + 12C_k - 6C_{k-1/2}\right) + \left(w_k C_{k+1/2} - w_k C_{k-1/2}\right)}{D_{x,k}h_k}. \tag{A.2c}$$

For the kth layer, the relation between the central node i, j and eight neighboring nodes at time step $(n+1)$ can be obtained

$$C_{i,j,k}^{n+1} = \left(C_{ne}C_{i+1,j+1,k}^{n+1} + C_{nw}C_{i-1,j+1,k}^{n+1} + C_{se}C_{i+1,j-1,k}^{n+1} + C_{sw}C_{i-1,j-1,k}^{n+1} + C_{wc}C_{i-1,j,k}^{n+1} + C_{ec}C_{i+1,j,k}^{n+1} \right.$$

$$\left. + C_{nc}C_{i,j+1,k}^{n+1} + C_{sc}C_{i,j-1,k}^{n+1} + \frac{R}{\Delta t}C_p C_{i,j,k}^n - C_p f_p \right) \bigg/ \left(1 + \frac{R}{\Delta t}C_p\right), \tag{A.3}$$

in which

$$C_{ec} = EBe^{-Ah}, \quad C_{ne} = Ee^{-Ah-Bk}, \quad C_{wc} = EBe^{Ah}, \quad C_{nw} = Ee^{Ah-Bk},$$

$$C_{sc} = EAe^{Bk}, \quad C_{se} = Ee^{-Ah+Bk}, \quad C_{nc} = EAe^{-Bk}, \quad C_{sw} = Ee^{Ah+Bk},$$

$$C_p = \frac{1}{2(A^2 + B^2C)}\left[(C_{nw} + C_{wc} + C_{sw} - C_{ne} - C_{ec} - C_{se})Ah\right.$$

$$\left. + (C_{sw} + C_{sc} + C_{se} - C_{nw} - C_{nc} - C_{ne})Bk\right],$$

$$E = \frac{1}{4\cosh(Ah)\cosh(Bk)} - E_2 Ah\coth(Ah) - BkE_2^*\coth(Bk),$$

$$EA = 2Ah\frac{\cosh^2(Ah)}{\sinh(Ah)}E_2, \quad EB = 2Bk\frac{\cosh^2(Bk)}{\sinh(Bk)}E_2^*,$$

$$E_2 = \frac{k^2}{Ch^2}E_2^* + \frac{BCh\tanh(Ah) - Ak\tanh(Bk)}{4ABCh^2\cosh(Ah)\cosh(Bk)}, \quad E_2^* = \sum_{m=1}^{\infty}\frac{-(-1)^m(\lambda_m k)}{\left[(Bk)^2 + (\lambda_m^* k)^2\right]^2\cosh\mu_m^* h},$$

$$\mu_m^* = (A^2 + B^2 C + \lambda_m^{*2}C)^{\frac{1}{2}}, \quad m = 1,2,3,\cdots,$$

$$\lambda_m^* = \frac{(2m-1)\pi}{2k}, \quad m = 1,2,3,\cdots,$$

where h and k are space steps in the x and y directions, respectively; Δt is time step; C_{ne}, C_{nw}, C_{se}, C_{sw}, C_{wc}, C_{ec}, C_{nc}, C_{sc} and C_p are the FA coefficients.

Eq. (3.1) in the text can be obtained by grouping all the undetermined variables appearing in Eq. (A.3) to the left-hand-side of the equation.

References

[1] A. N. S. AL-NIAMI AND K. R. RUSHTON, *Dispersion in stratified porous-media-analytical solutions*, Water Resour Res., 15(5) (1979), pp. 1044–1048.

[2] C. J. CHEN, H. NASERI-NESHAT AND K. S. HO, *Finite-analytic numerical solution of heat transfer in two-dimensional cavity flow,* Numer. Heat Trans., 4(2) (1981), pp. 179–197.

[3] Y. M. CHEN, H. J. XIE, H. KE AND R. P. CHEN, *An analytical solution for one-dimensional contaminant diffusion through multi-layered system and its applications*, Environ. Geol., 58(5) (2009), pp. 1083–1094.

[4] S. DIDIERJEAN, D. MAILLET AND C. MOYNE, *Analytical solutions of one-dimensional macrodispersion in stratified porous media by the quadrupole method: Convergence to an equivalent homogeneous porous medium*, Adv. Water Resour., 27(6) (2004), pp. 657–667.

[5] M. C. HUNG, T. Y. HSIEH, T. L. TSAI AND J. C. YANG, *A layer-integrated approach for shallow water free-surface flow computation*, Commun. Numer. Meth. Eng., 24(12) (2008), pp. 1699–1722.

[6] J. C. HWANG, C. J. CHEN, M. SHEIKHOSLAMI AND B. K. PANIGRAHI, *Finite analytic numerical-solution for two-dimensional groundwater solute transport*, Water Resour Res., 21(9) (1985), pp. 1354–1360.

[7] C. K. KIM AND J. S. LEE, *A 3-dimensional P_C-based hydrodynamic model using an ADI scheme*, Coast Eng., 23(3-4) (1994), pp. 271–287.

[8] Y. C. KUO, L. H. HUANG AND T. L. TSAI, *A hybrid three-dimensional computational model of groundwater solute transport in heterogeneous media*, Water Resour. Res., 44(3) (2008).

[9] C. J. LAI AND C. W. YEN, *Turbulent free-surface flow simulation using a multilayer model*, Int. J. Numer. Meth. Fl., 16(11) (1993), pp. 1007–1025.

[10] R. W. LARDNER AND H. M. CEKIRGE, *A new algorithm for 3-dimensional tidal and storm-surge computations*, Appl. Math. Model., 12(5) (1988), pp. 471–481.

[11] F. J. LEIJ AND M. T. VANGENUCHTEN, *Approximate analytical solutions for solute transport in 2-layer porous-media*, Transport Porous Med., 18(1) (1995), pp. 65–85.

[12] C. W. LI AND J. GU, *3d layered-integrated modelling of mass exchange in semi-enclosed water bodies*, J. Hydraul. Res., 39(4) (2001), pp. 403–411.

[13] Y. C. LI AND P. J. CLEALL, *Analytical solutions for contaminant diffusion in double-layered porous media*, J. Geotech. Geoenviron., 136(11) (2010), pp. 1542–1554.

[14] Y. S. LI AND J. M. ZHAN, *An efficient 3-dimensional semiimplicit finite-element scheme for simulation of free-surface flows*, Int. J. Numer. Meth. Fl., 16(3) (1993), pp. 187–198.

[15] L. LIN, J. Z. YANG, B. ZHANG AND Y. ZHU, *A simplified numerical model of 3-d groundwater and solute transport at large scale area*, J. Hydrodyn., 22(3) (2010), pp. 319–328.

[16] W. L. LIN, Y. HAIK, R. BERNATZ AND C. J. CHEN, *Finite analytic method and its applications: A review*, Dynam. Atmos Oceans, 27(1-4) (1998), pp. 17–33.

[17] C. X. LIU, W. P. BALL AND J. H. ELLIS, *An analytical solution to the one-dimensional solute advection-dispersion equation in multi-layer porous media*, Transport Porous Med., 30(1) (1998), pp. 25–43.

[18] C. X. LIU, J. E. SZECSODY, J. M. ZACHARA AND W. P. BALL, *Use of the generalized integral transform method for solving equations of solute transport in porous media*, Adv. Water Resour., 23(5) (2000), pp. 483–492.

[19] G. LIU AND B. C. SI, *Analytical modeling of one-dimensional diffusion in layered systems with position-dependent diffusion coefficients*, Adv. Water Resour., 31(2) (2008), pp. 251–268.

[20] C. J. NEVILLE, Compilation of Analytical Solutions for Solute Transport in Uniform Flow, S. S. Padadopulos & Associateds, Bethesda, MD, 1994.

[21] M. REGGIO, A. HESS AND A. ILINCA, *3-d multiple-level simulation of free surface flows*, J. Hydraul. Res., 40(4) (2002), pp. 413–423.

[22] E. A. SUDICKY, R. W. GILLHAM AND E. O. FRIND, *Experimental investigation of solute transport in stratified porous-media. 1. The nonreactive case*, Water Resour Res., 21(7) (1985), pp. 1035–1041.

[23] A. E. TAIGBENU AND O. O. ONYEJEKWE, *A flux-correct green element model of quasi three-dimensional multiaquifer flow*, Water Resour Res., 36(12) (2000), pp. 3631–3640.

[24] Y. TANG AND M. M. ARAL, *Contaminant transport in layered porous-media. 1. General-solution*, Water Resour Res., 28(5) (1992), pp. 1389–1397.

[25] T. L. TSAI, J. C. YANG AND L. H. HUANG, *An accurate integral-based scheme for advection-diffusion equation*, Commun. Numer. Meth. Eng., 17(10) (2001), pp. 701–713.

[26] W. F. TSAI AND C. J. CHEN, *Unsteady finite-analytic method for solute transport in groundwater-flow*, J. Eng. Mech-Asce., 121(2) (1995), pp. 230–243.

[27] W. F. TSAI, T. H. LEE, C. J. CHEN, S. J. LIANG AND C. C. KUO, *Finite analytic model for flow and transport in unsaturated zone*, J. Eng. Mech-Asce., 126(5) (2000), pp. 470–479.

[28] C. L. XIA AND Y. C. JIN, *Multilayer averaged and moment equations for one-dimensional open-channel flows*, J. Hydraul. Eng-Asce., 132(8) (2006), pp. 839–849.

[29] A. YAKIREVICH, V. BORISOV AND S. SOREK, *A quasi three-dimensional model for flow and transport in unsaturated and saturated zones: 1. Implementation of the quasi two-dimensional case*, Adv. Water Resour., 21(8) (1998), pp. 679–689.

[30] H. B. ZHAN, Z. WEN AND G. Y. GAO, *An analytical solution of two-dimensional reactive solute transport in an aquifer-aquitard system*, Water Resource Res., 45 (2009), pp. W10501.

[31] H. B. ZHAN, Z. WEN, G. H. HUANG AND D. M. SUN, *Analytical solution of two-dimensional solute transport in an aquifer-aquitard system*, J. Contam. Hydrol., 107(3-4) (2009), pp. 162–174.

[32] C. B. ZHAO, T. P. XU AND S. VALLIAPPAN, *Numerical modeling of mass-transport problems in porous-media-a review*, Comput. Struct., 53(4) (1994), pp. 849–860.